Optics Letters

Generating bona fide twisted Gaussian Schell-model beams

HAIYUN WANG,[1] XIAOFENG PENG,[1] LIN LIU,[1,5] FEI WANG,[1,6] YANGJIAN CAI,[1,2,7] AND SERGEY A. PONOMARENKO[3,4]

[1]School of Physical Science and Technology, Soochow University, Suzhou 215006, China
[2]Shandong Provincial Engineering and Technical Center of Light Manipulations & Shandong Provincial Key Laboratory of Optics and Photonic Device, School of Physics and Electronics, Shandong Normal University, Jinan 250014, China
[3]Department of Electrical and Computer Engineering, Dalhousie University, Halifax, Nova Scotia B3J2X4, Canada
[4]Department of Physics and Atmospheric Science, Dalhousie University, Halifax, Nova Scotia B3H 4R2, Canada
[5]e-mail: liulin@suda.edu.cn
[6]e-mail: fwang@suda.edu.cn
[7]e-mail: yangjiancai@suda.edu.cn

Received 17 June 2019; revised 29 June 2019; accepted 29 June 2019; posted 1 July 2019 (Doc. ID 370274); published 23 July 2019

We experimentally realize bona fide twisted Gaussian Schell-model (TGSM) beams by converting an anisotropic GSM beam into a TGSM beam with a set of just three cylindrical lenses. In contrast to the previously reported experimental technique for generating TGSM beams, we are able to explicitly generate anisotropic GSM beams with simultaneously controlled beam widths and transverse coherence lengths along two mutually orthogonal directions, prior to converting them to genuine TGSM beams.

https://doi.org/10.1364/OL.44.003709

In 1993, Simon and Mukunda introduced a twist phase concept for partially coherent beams and theoretically described a class of such beams with a twist phase, namely, twisted Gaussian Schell-model (TGSM) beams [1]. The twist phase fundamentally differs from the usual curvature phase of a Gaussian beam because the magnitude of the twist phase parameter is bounded by the inverse square of the transverse coherence length of the beam field onto which the twist phase is imparted. Thus, the twist phase exists only for partially coherent beams, and it vanishes in the fully coherent limit [1,2]. In addition, the twist phase has intrinsic chirality or handedness, which is responsible for the beam spot rotation during free-space propagation of the TGSM beam. The coherent mode decomposition of the cross-spectral density (CSD) of a TGSM source helps in gaining much physical insight into the nature of the beams generated by TGSM sources [3–5].

To date, the twist phase has arisen in many areas of optical physics. For instance, partially coherent optical solitons in certain slowly responding nonlinear media have been shown to possess a twist phase [5,6] that strongly affects their polarization properties [6]. Further, propagation properties of TGSM beams through a paraxial optical system, turbulent atmosphere, linear dispersive/absorbing media, and uniaxial crystals have been comprehensively examined [7–10]. It was found that imparting a twist phase on a partially coherent beam at the source can reduce the magnitude of turbulence-induced scintillations of the beam intensity at the receiver [11]. In addition, the Rayleigh limit in classical imaging systems can be overcome if one uses TGSM light beams for object illumination [12].

Yet despite impressive recent progress in theoretical understanding of the twist phase and the way it can be imparted on a wide class of partially coherent beams [13–18], the experimental demonstration of twisted beams presents a formidable challenge. To our knowledge, only Friberg *et al.* have so far reported the transformation of anisotropic (elliptical) GSM (AGSM) beams into TGSM beams using a six-cylindrical-lens (CL) optical system [2]. However, in their experiment, three uncorrelated elliptical Gaussian beams were used instead of an actual AGSM beam as input to their six-CL conversion system. Hence, the twisted beams realized in [2] are not, strictly speaking, bona fide TGSM beams.

In this Letter, we propose a three-CL system to transform an AGSM beam into a TGSM beam using Wigner distribution properties. We introduce an experimental setup to simultaneously control the AGSM beam widths and transverse coherence lengths in two orthogonal directions. We then demonstrate experimentally a successful transformation of the generated AGSM beam into a genuine TGSM beam using the three-CL system and study free-space propagation characteristics of the obtained TGSM beam.

The CSD function of a TGSM source at the points specified by $\mathbf{r}_1$ and $\mathbf{r}_2$ is expressed as [1]

$$W_0(\mathbf{r}_1,\mathbf{r}_2) = \exp\left[-\frac{(\mathbf{r}_1^2+\mathbf{r}_2^2)}{4\omega_0^2}\right]\exp\left[-\frac{(\mathbf{r}_1-\mathbf{r}_2)^2}{2\delta_0^2}\right] \times \exp[-ik\mu_0(\mathbf{r}_1\times\mathbf{r}_2)_\perp], \tag{1}$$

where $k = 2\pi/\lambda$ is the wave number with λ being the wavelength of light; ω_0 and δ_0 denote the beam width and transverse coherence length, respectively. The subscript "⊥" denotes the cross-product component orthogonal to the mean propagation axis; μ_0 is a twist parameter measuring the twist phase magnitude. The magnitude of μ_0 is bounded from above as $|\mu_0| \leq (k\delta_0^2)^{-1}$, ensuring the non-negative definiteness of the CSD function.

Hereafter, it will prove convenient to introduce the Wigner distribution function defined as

$$W(\mathbf{r},\mathbf{p}) = \left(\frac{k}{2\pi}\right)^2 \iint W_0\left(\mathbf{r}+\frac{\mathbf{r}'}{2},\mathbf{r}-\frac{\mathbf{r}'}{2}\right)\exp(ik\mathbf{p}\cdot\mathbf{r}')\mathrm{d}\mathbf{r}', \tag{2}$$

where $\mathbf{r} = (\mathbf{r}_1+\mathbf{r}_2)/2$, $\mathbf{r}' = \mathbf{r}_1 - \mathbf{r}_2$. After substituting from Eq. (1), integrating over $\mathbf{r}'$, and rearranging terms, Eq. (2) takes the form

$$W(\xi) = \frac{1}{(2\pi)^2}(\det V')^{-1/2}\exp\left(-\frac{1}{2}\xi^T V'^{-1}\xi\right), \tag{3}$$

where $\xi^T = (\mathbf{r}^T, \mathbf{p}^T)$ is a column matrix; $\mathbf{r}$ and $\mathbf{p}$ represent the position and the direction variables, respectively. Hence, the TGSM beam is fully characterized by a variance matrix V':

$$V' = \begin{bmatrix} \Omega_0\kappa & 0 & 0 & \upsilon_0 \\ 0 & \Omega_0\kappa & -\upsilon_0 & 0 \\ 0 & -\upsilon_0 & \Omega_0^{-1}\kappa & 0 \\ \upsilon_0 & 0 & 0 & \Omega_0^{-1}\kappa \end{bmatrix}, \tag{4}$$

where

$$\begin{aligned} \Omega_0 &= \left[\frac{1}{k^2\omega_0^2}\left(\frac{1}{4\omega_0^2}+\frac{1}{\delta_0^2}\right)+\mu_0^2\right]^{-\frac{1}{2}}, \\ \kappa &= \omega_0^2\left[\frac{1}{k^2\omega_0^2}\left(\frac{1}{4\omega_0^2}+\frac{1}{\delta_0^2}\right)+\mu_0^2\right]^{\frac{1}{2}}, \\ \upsilon_0 &= \mu_0\omega_0^2. \end{aligned} \tag{5}$$

Note that the Wigner and CSD distributions have identical information content. According to the Williamson theorem [3], a variance matrix of the beam field, transmitted through a first-order optical system, satisfies the relation $V' = \mathbf{S}V\mathbf{S}^T$, where V is a variance matrix of the beam field in the source plane, and $\mathbf{S}$ is a 4×4 ray transfer matrix of the optical system; the superscript "T" denotes matrix transposition.

To figure out how to synthesize a TGSM beam, we start with an AGSM source beam with the variance matrix as

$$V = \begin{bmatrix} \Omega_0(\kappa-\upsilon_0) & 0 & 0 & 0 \\ 0 & \Omega_0(\kappa+\upsilon_0) & 0 & 0 \\ 0 & 0 & \Omega_0^{-1}(\kappa-\upsilon_0) & 0 \\ 0 & 0 & 0 & \Omega_0^{-1}(\kappa+\upsilon_0) \end{bmatrix}. \tag{6}$$

The CSD function of the ASGM source then reads

$$W_0(x_1,y_1;x_2,y_2;0) = \exp\left(-\frac{x_1^2+x_2^2}{4\omega_{0x}^2}-\frac{y_1^2+y_2^2}{4\omega_{0y}^2}\right) \times\exp\left[-\frac{(x_1-x_2)^2}{2\delta_{0x}^2}-\frac{(y_1-y_2)^2}{2\delta_{0y}^2}\right], \tag{7}$$

where we introduce the notations

$$\begin{aligned} &\omega_{0x}^2 = \Omega_0(\kappa-\upsilon_0), \qquad \omega_{0y}^2 = \Omega_0(\kappa+\upsilon_0), \\ &\delta_{0x}^{-2} = k^2\Omega_0^{-1}(\kappa-\upsilon_0) - (4\omega_{0x}^{-2}), \\ &\delta_{0y}^{-2} = k^2\Omega_0^{-1}(\kappa+\upsilon_0) - (4\omega_{0y}^2)^{-1}. \end{aligned} \tag{8}$$

In Eq. (8), $\omega_{0\alpha}$ and $\delta_{0\alpha}$ ($\alpha = x, y$) are, respectively, the beam width and transverse coherence length of the AGSM beam along the α direction. Now, the task is to find a ray transfer matrix corresponding to V' of a TGSM beam. In principle, the solution for $\mathbf{S}$ is not unique. Simon *et al.* [1] obtained a solution $\mathbf{S}$ that was subsequently utilized by Friberg *et al.* in their experimental realization of TGSM beams with the aid of a set of six CLs. We find an alternative solution for $\mathbf{S}$ in the form

$$\mathbf{S} = -\frac{1}{2}\begin{bmatrix} 1 & 1 & -\Omega_0 & \Omega_0 \\ 1 & 1 & \Omega_0 & -\Omega_0 \\ 1/\Omega_0 & -1/\Omega_0 & 1 & 1 \\ -1/\Omega_0 & 1/\Omega_0 & 1 & 1 \end{bmatrix}. \tag{9}$$

To experimentally realize the transfer matrix of Eq. (9), we use a set of three CLs shown in part II of Fig. 1. The focal lengths of CL_1, CL_2, and CL_3 are $f/2$, f, and $f/2$, respectively. The three lenses CL_1, CL_2, CL_3 as well as the A-A and B-B planes are placed with an interval of $f/2$ apart from each other. Hence, CL_1 and CL_3 form a standard $4f$ imaging system, and CL_2 performs a Fourier transform in a direction orthogonal to either CL_1 or CL_3. Moreover, the optical axes of CL_1 and CL_3 make an angle $-\pi/4$ with respect to the y axis, and the CL_2 axis is orthogonal to the CL_1 or CL_3 axis. Next, the transfer matrix of a single CL with its axis making an angle θ with the y axis, reads [19]

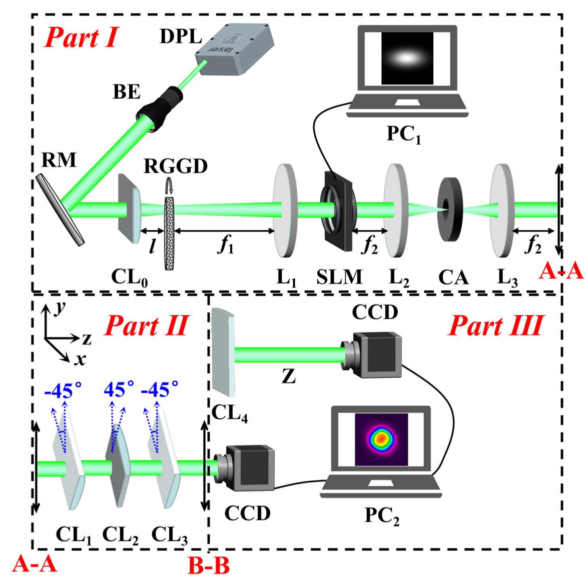

Fig. 1. Experimental setup for generating a TGSM beam. DPSS, diode-pumped solid-state laser; BE, beam expander; RM, reflecting mirror; CL_0, CL_1, CL_2, CL_3, and CL_4, thin cylindrical lenses; RGGD, rotating ground glass disk; L_1, L_2, and L_3, thin lenses; SLM, spatial light modulator; CA, circular aperture; CCD, charge-coupled device; PC_1 and PC_2, personal computers.

$$L(f,\theta)=\begin{bmatrix}\mathbf{I} & \mathbf{0}\\ \Phi & \mathbf{I}\end{bmatrix}, \tag{10}$$

with

$$\Phi=\frac{1}{f}\begin{bmatrix}-\cos^2\theta & \sin\theta\cos\theta\\ \sin\theta\cos\theta & -\sin^2\theta\end{bmatrix}. \tag{11}$$

In Eq. (10), $\mathbf{0}$ and $\mathbf{I}$ stand for 2×2 null and unit matrices. The free-space transfer matrix over a distance d is given by

$$D(d)=\begin{bmatrix}\mathbf{I} & d\mathbf{I}\\ \mathbf{0} & \mathbf{I}\end{bmatrix}. \tag{12}$$

The transfer matrix $\Gamma(f)$ of the system follows from Eqs. (10)–(12):

$$\begin{aligned}\Gamma(f) &= D(f/2)L(f/2,\,-\pi/4)D(f/2)\\ &\quad\times L(f,\pi/4)D(f/2)L(f/2,\,-\pi/4)D(f/2)\\ &= -\frac{1}{2}\begin{pmatrix}1 & 1 & -f & f\\ 1 & 1 & f & -f\\ 1/f & -1/f & 1 & 1\\ -1/f & 1/f & 1 & 1\end{pmatrix}.\end{aligned} \tag{13}$$

We can infer at once by comparing Eqs. (9) and (13) that if we set $f=\Omega_0$, the CL set of part II in Fig. 1 transforms an AGSM beam into a TGSM beam with the parameters determined from Eq. (8).

In part I in Fig. 1, we exhibit an experimental setup for generating the AGSM beam with prescribed parameters. A linearly polarized laser beam ($\lambda=532$ nm), generated by a diode-pumped solid-state (DPSS) laser, was expanded by a beam expander (BE), reflected by a mirror, and transmitted through a thin CL, CL_0. The transmitted beam was then incident onto a rotating ground glass disk (RGGD). We can regard the light transmitted through the RGGD as spatially incoherent if the diameter of the beam spot on the RGGD is larger than the inhomogeneity scale of the ground glass; this condition was satisfied in our case. Past the RGGD, the light beam was collimated by a thin lens L_1 with focal length $f_1=35$ cm, generating a partially coherent beam with a uniform intensity and elliptically anisotropic Gaussian degree of coherence. According to the van Cittert–Zernike theorem, the transverse coherence widths of the generated beam along the x and y directions are $\delta_{0x}=\lambda f_1/\pi\omega_{sx}$, $\delta_{0y}=\lambda f_1/\pi\omega_{sy}$, respectively, $\omega_{sx(y)}$ being the beam widths along the x, y directions in the RGGD plane. In the experiment, we controlled the beam widths ω_{sx} and ω_{sy} by adjusting the magnification of the BE and the distance between the CL_0 and RGGD. Thus, we were able to adjust the coherence lengths of the beam in two mutually orthogonal directions. We then employed a spatial light modulator (SLM), placed in front of L_1, to convert a uniform intensity profile to an elliptical Gaussian shape. The beam widths were precisely controlled by the hologram loaded onto the SLM. Further, the circular aperture lenses L_2 and L_3 with focal lengths $f_2=f_3=15$ cm formed a $4f$ spatial filter to remove the unwanted diffraction orders introduced by the SLM. This procedure yielded an ASGM beam with controlled widths and coherence lengths in the A-A plane.

As an example, we preset the AGSM beam parameters at $\omega_{0x}=0.37$ mm, $\omega_{0y}=0.18$ mm, $\delta_{0x}=0.046$ mm, $\delta_{0y}=0.10$ mm. This parameter set satisfies Eq. (8) if we choose $f=\Omega_0=20$ cm and $\mu_0=0.003\ (\mathrm{mm})^{-1}$. In Fig. 2 we display the experimental results for the normalized intensity of the generated AGSM beam in the A-A plane. For comparison, the corresponding theoretical fits are also plotted in Fig. 2. It can be seen in Figs. 2(c) and 2(d) that the experimental results for the beam widths in the x or y directions agree well with our preset theoretical parameters. In Fig. 3, we show the experimental results and corresponding theoretical fits for the square of the AGSM beam degree of coherence in the A-A plane. The protocol we followed to measure the AGSM beam degree of coherence is described in [20]. It can be inferred from Fig. 3 that the degree of coherence has an anisotropic Gaussian shape with the prescribed coherence lengths along the x and y directions.

Once we had generated the AGSM beam using the optical system in part I, we transmitted the beam through the three CLs system, which transformed it into a TGSM beam in the B-B plane. Note that the A-A plane in part I (source plane of the AGSM beam) in Fig. 1 is the same as the A-A plane in part II. The focal lengths of CL_1, CL_2, and CL_3 were set to 10 cm, 20 cm, and 10 cm, respectively, matching Ω_0. We placed a CCD in the B-B plane to measure the TGSM beam intensity and degree of coherence distributions. In Fig. 4, we exhibit the experimental results for the normalized intensity distribution of the generated TGSM beam and the corresponding theoretical fits. As expected, the beam profile acquires a circular Gaussian shape. We can infer from the theoretical fits

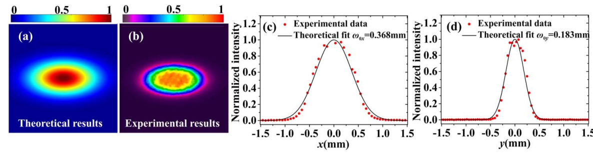

Fig. 2. Theoretical and experimental results for the normalized intensity distribution of the generated AGSM beam. Solid lines denote theoretical fits to the experimental results.

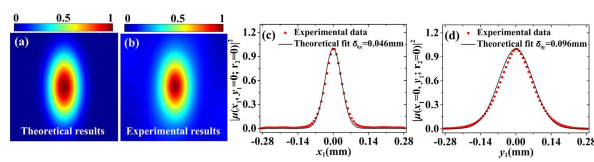

Fig. 3. Theoretical and experimental results for the square of the degree of coherence of the generated AGSM beam. Solid lines denote theoretical fits to the experimental results.

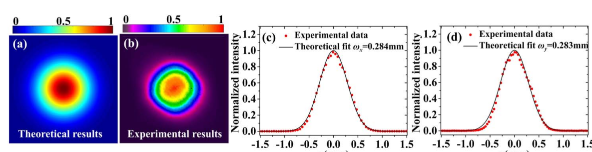

Fig. 4. Theoretical and experimental results for the normalized intensity distribution of the generated (isotropic) TGSM beam in the B-B plane in Fig. 1. Solid lines display theoretical fits to the experimental results.

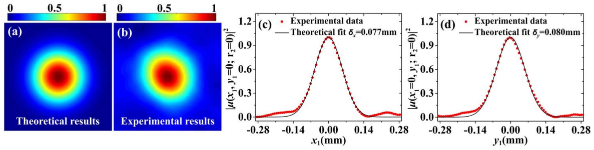

Fig. 5. Theoretical and experimental results for the square of the degree of coherence of the generated (isotropic) TGSM beam in the B-B plane in Fig. 1. Solid lines display theoretical fits to the experimental results.

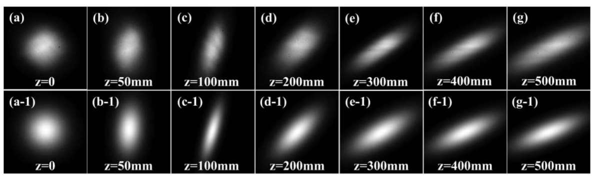

Fig. 6. Experimental (first row) and theoretical (second row) results for the normalized intensity distribution of the TGSM beam transmitted through a thin cylindrical lens CL_4 at several propagation distances behind the lens.

that the realized beam widths in the x and y directions are both about 0.28 mm, which is in reasonable agreement with the theoretical prediction of 0.29 mm. In Fig. 5, we display the square of the TGSM beam degree of coherence. Through a theoretical fit to the experimental data, we obtain the transverse coherence lengths of $\delta_x = 0.077$ mm and $\delta_y = 0.080$ mm, while the theory predicts $\delta_{x(y)} = 0.074$ mm. The small discrepancy between the theory and experiment can be explained by small calibration errors in determining the separation distances between and rotation angles of the three CLs. In general, our experimental results are very consistent with the theoretical analysis, and the proposed three-CL optical system is adequate for generating bona fide TGSM beams.

The twist phase is known to be responsible for the beam spot rotation on free-space propagation. However, the spot rotation cannot be directly observed due to the circular symmetry of the TGSM beam cross section. To verify the twist phase existence, we then placed another CL, CL_4, with focal length 10 cm in the B-B plane—shown in part III in Fig. 1—and recorded the intensity evolution of the TGSM beam transmitted through CL_4 on its subsequent propagation.

In Figs. 6(a)–6(g), we illustrate the experimentally obtained intensity distributions of the TGSM beam at several propagation distances. For comparison, the corresponding simulation results are plotted in Figs. 6(a-1)–6(g-1). We can infer from Fig. 6 that the beam spot rotates clockwise with respect to the propagation axis due to the twist phase presence, thereby directly revealing the twist phase. The beam spot rotated by the angle of 45 deg over the propagation distance $z = 200$ mm. The experimental results are in excellent agreement with the simulations. We note in conclusion that if one rotates all three CLs by 90 deg, the beam spot rotation direction is reversed.

In summary, we have proposed a three-CL optical system to transform an AGSM beam to a TGSM beam. To generate a bona fide TGSM beam, the AGSM beam widths and transverse coherence lengths should be precisely controlled. To this end, we proposed an experimental setup to simultaneously control the AGSM beam widths and transverse coherence lengths in two mutually orthogonal directions. We then converted the controlled AGSM beam into a TGSM beam. Our work may be useful for generating other types of twisted beams, and we expect it to stimulate further experimental studies of twisted beams.

Funding. National Natural Science Foundation of China (NSFC) (11525418, 11774251, 11874046, 91750201); Priority Academic Program Development of Jiangsu Higher Education Institutions; Qing Lan Project of Jiangsu Province; Natural Sciences and Engineering Research Council of Canada (NSERC) (RGPIN-2018-05497).

REFERENCES

1. R. Simon and N. Mukunda, J. Opt. Soc. Am. A **10**, 95 (1993).
2. A. T. Friberg, E. Tervonen, and J. Turunen, J. Opt. Soc. Am. A **11**, 1818 (1994).
3. K. Sundar, N. Mukunda, and R. Simon, J. Opt. Soc. Am. A **12**, 560 (1995).
4. D. Ambrosini, V. Bagini, F. Gori, and M. Santarsiero, J. Mod. Opt. **41**, 1391 (1994).
5. S. A. Ponomarenko, Phys. Rev. E **64**, 036618 (2001).
6. S. A. Ponomarenko and G. P. Agrawal, Phys. Rev. E **69**, 036604 (2004).
7. Q. Lin and Y. Cai, Opt. Lett. **27**, 216 (2002).
8. Y. Cai and S. He, Appl. Phys. Lett. **89**, 041117 (2006).
9. Y. Cai, Q. Lin, and D. Ge, J. Opt. Soc. Am. A **19**, 2036 (2002).
10. L. Liu, Y. Chen, L. Guo, and Y. Cai, Opt. Express **23**, 12454 (2015).
11. F. Wang, Y. Cai, H. T. Eyyuboğlu, and Y. Baykal, Opt. Lett. **37**, 184 (2012).
12. Z. Tong and O. Korotkova, Opt. Lett. **37**, 2595 (2012).
13. R. Borghi, F. Gori, G. Guattari, and M. Santarsiero, Opt. Lett. **40**, 4504 (2015).
14. F. Gori and M. Santarsiero, Opt. Lett. **40**, 1587 (2015).
15. Z. Mei and O. Korotkova, Opt. Lett. **42**, 255 (2017).
16. F. Gori and M. Santarsiero, Opt. Lett. **43**, 595 (2018).
17. L. Wan and D. Zhao, Opt. Lett. **43**, 3554 (2018).
18. X. Peng, L. Liu, F. Wang, P. Sergei, and Y. Cai, Opt. Express **26**, 33956 (2018).
19. A. E. Attard, Appl. Opt. **23**, 2706 (1984).
20. F. Wang, X. Liu, Y. Yuan, and Y. Cai, Opt. Lett. **38**, 1814 (2013).